

# Modeling the Propagation of Ultrasonic Waves in a Medium with Non-homogeneities

Mitko MIHOVSKI, Alexander ALEXIEV, Boris KOVACHEV, Borislav KIROV, Yordan MIRCHEV, Yonka IVANOVA, Institute of Mechanics-Bulgarian Academy of Sciences, Sofia, Bulgaria

**Abstract.** A unified approach to the modeling of the propagation of acoustic waves is developed in the present paper. It is based on the acoustic tract analysis. The sample model problems solved by using the proposed approach are: study of a reversible quartz transducer, study of the spectrum of reflection from model reflectors, study of a layered composite, estimation of the conventional dimensions of non-homogeneities, modeling of the propagation of an ultrasonic impulse in powder-metallurgical materials, modeling the propagation of ultrasonic waves in cast iron containing spheroid graphite particles, modeling of reflection from rough surfaces and application of the method of spectral analysis in the investigation of material structure.

The development of theoretical and experimental studies and methods of computer modeling provides significant possibilities to investigate the ultrasonic wave propagation and interaction with material and product non-homogeneities, [1]-[3]. The aim of the present study is to present part of the investigations in the field, performed in the Laboratory of Mechanics, Diagnostics and Non-destructive Testing at the Institute of Mechanics, Bulgarian Academy of Sciences.

## 1. An Acoustic Tract Involved in Ultrasonic Testing

A unified approach to the modeling of the propagation of acoustic waves is developed in the present paper. It is based on the acoustic tract analysis performed in Ref. [1] and further developed in Refs. [2] and [3]. A sample generalized form of the acoustic tract when employing the echo-impulse method reads:

$$(1) A(x, t) = A_0(0, t) \left[ \prod_{i=1}^n e^{-2\alpha_i x_i} \right] \left[ \prod_{i=1}^m D_{i,i+1} D_{i+1,i} \right] \Phi_H Q_A R$$

The following notations are used in the above formula:  $A_0(0, t)$  and  $A(x, t)$  are the emitted and received ultrasonic signals, respectively;  $\alpha_i$  is the attenuation coefficient;  $x_i$  is the acoustic path within a medium  $i$ ,  $D_{i,i+1}$  is an amplitude coefficient of permeability of the interface between medium  $i$  and medium  $i + 1$ ,  $\Phi_H$  is a function which accounts for the direction characteristics of the sensor under emitting and receiving regimes;  $Q_A$  is a function which accounts for the reflector capabilities;  $R$  is a coefficient of reflection from the basic reflecting

surface and  $i$  is an index of the medium which the ultrasonic waves propagate in.

All cases considered below employ the echo-impulse method. It is assumed that the impulse signals act on the piezo-plate of the sensor. The signals have a bell shaped envelope and they are introduced by means of the following expression:

$$(2) A_o(0, t) = A_o \exp(j\omega t - \delta_o^2 t^2)$$

Here  $A_o$  is the maximal amplitude of the emitted signals ( $A_o=1$ ),  $\omega$  is the angular frequency,  $\delta_o$  is a coefficient of the impulse shape,  $\delta_o = (2f_o\sqrt{\ln 2})/n_o$ ,  $f_o$  is the operation frequency,  $n_o$  is the number of oscillations at a level equal to  $A_o/2$ . The signal spectrum is given in the form

$$(3) S_o(0, \omega) = \frac{1}{2\pi} \int_{-\infty}^{+\infty} A(0, t) e^{-j\omega t} dt$$

The acoustic signal  $A(x, t)$  registered during test performance and having covered a distance  $x$  within the material is presented as

$$(4) A(x, t) = \frac{1}{2\pi} \int_{-\infty}^{+\infty} S(x, \omega) e^{-j\omega t} d\omega$$

where  $S(x, \omega) = S(0, \omega) \left[ \prod_{i=1}^k F_i \right]$  and  $F_i$  are functions that consider effects of the emitting-receiving system, contact conditions, medium characteristics, object non-homogeneities and wave reflectors located within the object.

The following informative characteristics are used in test practice: distance to the non-homogeneities, amplitude of the reflected signal, characteristics of the spectrum obtained by using Fourier transformations.

## 2. Sample model problems solved by using the proposed approach

### 2.1. Study of a reversible quartz transducer

Assume that the material subjected to ultrasonic treatment has a minimal attenuation and the coefficient of reflection is  $R = 1$ . The frequency characteristic of the sensor is given in the form [4]

$$(5) F_1(\omega) = \frac{1}{2} \sqrt{\frac{(1 - \cos y)^2 + (z_2/z_1)^2 \sin^2 y}{A^2 + B^2}}$$

where  $A = (z_2/z_e + z_1/z_2) \sin y \cos y_2 + (z_3/z_e + z_1/z_3) \cos y \sin y_2$ ,

$$B = (1 + z_1/z_e) \cos y \cos y_2 + (z_2/z_3 - z_3/z_e) \sin y \sin y_2,$$

$$z_e = z_4(z_5 - iz_4 \operatorname{tg}(k_5 d)) / (z_5 - iz_5 \operatorname{tg}(k_5 d))$$

Note that  $z_1 - z_5$  are the acoustic impedances of the damper, piezo-element, protector, contact

layer and medium, respectively. Note also that  $y = \pi f / f_0$ ,  $y_2 = my$  and  $m = \frac{d_p}{\lambda}$  where  $d_p$  is the protector thickness,  $\lambda$  is the wave length,  $d$  is thickness of the contact layer and  $k_i$  is the wave number for the  $i$ -th medium.

Fig. 1 shows spectra of the electric bell-shaped signals, having frequency  $f_0 = 4$  MHz and oscillation number  $n_0 = 3, 5$  and  $7$  (curves S1, S2, S3), and normalized with respect to the spectrum of the impulse with  $n_0 = 7$ .

Fig. 2 shows normalized amplitude-frequency characteristics of the emitting-receiving system. The system has a quartz piezo-element with a basic resonance frequency  $f_0 = 4$  MHz and with acoustic damper resistance  $z = 25 \cdot 10^5$  ак.Ω, and the piezo-element operates over a steel specimen with  $z_5 = 32,2 \cdot 10^6$  ак.Ω. Curves S1, S2, S3 correspond to contact layers with thicknesses  $0,5 \lambda_4, 0,1 \lambda_4, 0,02 \lambda_4$ , respectively, where  $\lambda_4$  is the length of a wave propagating in water layer (with an acoustic resistance  $z_2 = 1,5 \cdot 10^6$  ак.Ω). The impacting radio-impulse is bell shaped with oscillation number  $n_0 = 5$ . Using this method, one can more precisely account for the effect of the emitting-receiving system and for that of the system elements. Thus, the accuracy of modeling the propagation of ultrasonic waves in the material increases.

## 2.2. Study of the spectrum of reflection from model reflectors

The study considers a model of the acoustic tract for a medium without attenuation and with model reflectors. The reflector types are as follows: infinite cylinder reflector (CR), flat-bottom cylindrical reflector (FBR), spherical reflector (SR) and infinite plane reflector (PR). Following [1], the reflection coefficients of those devices read as follows:

$$(6) R_{CR} = \frac{S}{\sqrt{8\lambda}} \sqrt{\frac{d}{X^3}}, R_{FBR} = \frac{S_o \pi d^2}{\lambda^2 X^2}, R_{CR} = \frac{S_d}{4\lambda X^2}, R_{(PR)} = \frac{S}{2\lambda X},$$

where  $S$  is the sensor area,  $d$  is the reflector diameter,  $\lambda$  is the wave length,  $c$  is the sound velocity and  $X$  is the “sensor-reflector” distance. Fig. 3 presents results of the calculations for  $f_0 = 4$  MHz,  $n_0 = 7$ , contact layer thickness  $0,1 \lambda_4$  and  $d = 5$  mm. Curves S1, S2, S3 and S4 correspond to an infinite plane and to a cylindrical, flat-bottom and spherical reflector, respectively.

Fig. 4 shows spectra of the reflected signals of the equivalent FBR and CR for the case of CR, with diameters 3, 4 and 5 mm (curves S3, S2 and S1 – solid lines) and of the equivalent FBR-s with diameters 2.99, 3, 2.13 and 3.397 mm (dashed lines). The diameters of the equivalent and flat-bottom reflectors are calculated using the relation

$$(7) d_{FBR} = \sqrt{\frac{\lambda \sqrt{2}}{\pi}} \sqrt{d_{CR} X},$$

for the case  $f_0 = 4$  MHz,  $n_0 = 7$  and contact layer thickness  $0,1 \lambda_4$ . Spectrum normalization is preformed with respect to the spectrum of the reflector  $d_{FBR} = 3.397$  mm. The calculations consider either the change of the signal spectrum or the direction characteristics of both the sensor and reflector. One can observe an insignificant change of the spectrum amplitude, as well as a displacement of the maximums towards lower frequencies for FBR-s that are equivalent with respect to CR.

## 2.3. Study of a layered composite

We consider testing of an immersion variant of a layered composite, accounting for a normal

incidence of an ultrasonic signal (Fig. 5). The reflection coefficient R is presented by means of the following relation, [5]

$$(8) \quad R = \frac{z_e^2 - z_5^2}{z_e^2 + z_5^2}$$

where  $z_e$  is the input resistance of the composite and  $z_5$  is the acoustic resistance of water.

The studied composite consists of three layers - aluminum with thickness  $d_4=1$  mm, adhesion layer-  $d_3=0.1$  mm and aluminum with thickness  $d_2=1$ mm. Spectra of reflected signals are calculated regarding the emission of an ultrasonic signal with  $f_0 = 4$  MHz and  $n_0=3$ . The results found (with and without layer) are plotted in Fig. 6 - curves S1 and S2, respectively. A significant change of the results is observed when replacing the adhesion layer with an air layer. The spectrum change control proves useful to control the quality of composite materials.

#### 2.4. Estimation of the conventional dimensions of non-homogeneities

The problem of modeling is presented in Fig. 7, where a disk sensor with frequency of 4 MHz and a non-axially located flat-bottom reflector (FBR) are used. The function that expresses the influence of the directivity of both the sensor and reflector, as well as their mutual location, has the form, [1]

$$(9) \quad \Phi_A = \frac{\lambda^2 r_s^2 r^2 f^2}{\lambda^2 X^2} \cos \delta |R(\delta)| \Phi^2(r_s k \sin \theta) \Phi'(rk \sin \delta)$$

Notations used in the above formula are as follows:  $\Phi(r_s k \sin \theta)$  and  $\Phi(r k \sin \theta)$  are the emitter and reflector directivity characteristics;  $r_s$  and  $r$  are the emitter and reflector radii;  $\delta$  is the incidence angle of the ultrasonic ray and  $R(\delta)$  is the coefficient of reflection from a flat-bottom cylindrical reflector.

Fig. 8 shows relations between the reflected signal amplitudes and distance  $p$ , where the solid line plots calculation results valid for the emission of an impulse with  $f_0 = 2$  MHz,  $n_0=3$ , FBR with  $r=2,5$  mm. The amplitudes are in relation with a signal corresponding to reflection from an infinite plane.

The dashed line plots subsequent experimental results, where tests are performed using an ultrasonic impulse defectoscope. Good qualitative agreement is observed. The model does not consider contact layer and emitting-receiving system effects.

#### 2.5. Modeling of the propagation of an ultrasonic impulse in powder-metallurgical materials

Ref. [2] illustrates that composite materials based on iron powder and prepared by using the methods of powder metallurgy can be successfully tested using ultrasonic methods. Based on models developed in [6]-[9], Ref. [1] proposes a relation for calculating the coefficient of attenuation within the material:

$$(10) \quad \alpha(f) = \alpha_k(f) + \alpha_p(f) + \alpha_r(f) + \alpha_m(f),$$

Notations  $\alpha_k, \alpha_p, \alpha_r, \alpha_m$  in the above formula express the effects of crystallites, pores, powder initial particles and contact between particles.

The following effects are usually considered in modeling the propagation of ultrasonic waves within a composite: distribution of crystallites and pores with respect to dimensions, average dimension of particles of the initial powder, mean quadratic deviation of the propagation velocity as dependent on crystal anisotropy and particle contact.

The results of modeling the propagation of waves within a composite prepared from iron powder type NC (Hoganes Company) are shown in Fig. 9 and Fig. 10. An impulse with frequency 4 MHz is used. A specimen with thickness 20 mm and porosity of 15 volume percents is ultrasonically treated, and the Weibull laws of statistical distribution of crystallite and pores are derived employing the methods of metallographic quantitative analysis, [2]. The mean dimensions of particles, crystallites and pores are 80, 35, 2  $\mu$  m, respectively.

Fig. 9 shows bottom signals A0 and A1 received from a material with zero attenuation and from a composite, respectively. Fig. 10 shows schematically the spectra of signals S0 and S1. Note that the significant changes of the amplitudes and spectra of the informative signal are useful for the performance of an acoustic analysis of the structure of powder-metallurgical materials. The comparison of spectra found by using different acoustic methods enables one to find the frequency dependence of  $\alpha$  when performing a single acoustic study. The change of  $n_0$  provides a possibility to regulate the characteristics of the emitted signal used in the acoustic analysis.

### *2.6. Modeling the propagation of ultrasonic waves in cast iron containing spheroid graphite particles*

The analysis of the structure of highly strong cast iron performed in Ref. [2] shows that cast iron is practically a composite ferrite-pearlite based material where the diameters of the spheroid graphite inclusions are statistically distributed according to Weibull's law. The attenuation coefficient is introduced by the relation

$$(11) \alpha = \alpha_M + \alpha_g,$$

where  $\alpha_M$  and  $\alpha_g$  denote the attenuation within the matrix and the scatter due to graphite.

Using classical theoretical relations for Rayleigh's scatter from crystallites and spheroid inclusions [2], [6], [7], [5], one could calculate those coefficients. Usually, calculations are performed using the mean diameter of graphite inclusions and crystallites, disregarding their statistical distributions. Moreover, no effects of multiple scatter from inclusions are considered. However, the proposed model of propagation of waves within highly strong cast iron considers those disregarded effects and provides higher result accuracy. It also takes into account the frequency characteristics of the emitting and receiving acoustic system.

Fig. 11 shows the calculated spectra of bottom signals, considering a mean inclusion diameter  $\overline{D_c} = 62 \mu$  m – curve SH, as well as the statistical distribution and multiple scatter from inclusions – curve SP. The emitted signal spectrum is denoted by SI.

A numerical experiment is performed, regarding the case of a damped transducer and an impulse with a carrying frequency 4 MHz and  $n_0=1$ , while the acoustic path within the specimen is 200 mm.

A number of essential phenomena are observed - decrease of the spectrum width, occurrence of non-symmetry and carrying frequency displacement to lower values. It seems reasonable to explain them with the significant impact of crystallites with dimensions larger than the mean one on attenuation.

Fig. 12 shows the shapes of impulses AI, AH, AP, corresponding to spectra SI, SH and SP. The durability of signal AH is the largest one and it is calculated using data for the mean inclusion diameter.

### 2.7. Modeling of reflection from rough surfaces

This paragraph treats a model problem of a flat wave reflection from model non-homogeneities, considering wave normal incidence. A normal roughness distribution is assumed in the model. A frequency dependence of the reflection coefficient of the following form is introduced, [11]

$$(12) \quad R = R_0 \cdot e^{-2 \cdot h^2 \cdot k_1^2},$$

Notations used are as follows:  $R_0$  is the coefficient of wave reflection from a smooth surface for wave normal incidence,  $h$  is the roughness height and  $k$  is the material wave number.

The effect of the wave attenuation within the material and the frequency-dependent coefficient of reflection are considered in the model design. The model capability is proved by testing a steel specimen with thickness of 28mm where the corrosion damage of the specimen surface varies from 0,1mm to 0,5mm. The acoustic impulse has parameters  $f_0=4\text{MHz}$ ,  $n_0=2$ . Fig. 13 shows spectra S1 and Sk of two signals A1 and Ak that are reflected from a smooth surface and a rough surface, respectively. Shapes A1 and Ak of the corresponding signals are found applying an inverse Fourier transformation and they are shown in Fig. 14. Signal Ak is amplified by 6dB for a better comparison, and  $t$  is time of signal propagation, measured in microseconds.

The following effects are registered: change of the shape of signals reflected from the rough surface, displacement of the begin of the signal from rough surface toward the signal from smooth surface, spectra displacement to lower frequencies.

## 3. Application of the method of spectral analysis in the investigation of material structure [10]

Objects of study are 6 series of specimens. Specimens are fabricated from carbon steel, being thermally treated to obtain a ferrite-pearlite structure with different grain size. Table 1 gives parameters of the thermal treatment (temperature  $T$  and duration  $t$ ) and the metallographic mean dimensions of the ferrite ( $D_f$ ) grains measured after the thermal treatment accomplishment.

Table 1

Series 20	$T$ , $^{\circ}\text{C}$	$t$ , h	$D_f$ , $\mu\text{m}$	$\alpha_1$ , Np/m.MHz	$\alpha_4$ , Np/m.MHz <sup>4</sup>
1	750	2	18	1,24	$1,68 \cdot 10^{-4}$
2	850	2	18	1,35	$1,5 \cdot 10^{-4}$
3	900	2	9	1,14	$2,197 \cdot 10^{-4}$
4	950	2	6	1,35	$5,23 \cdot 10^{-4}$
5	1000	10	42	2,4	$1,1 \cdot 10^{-4}$
6	1150	10	48	2,5	$1,39 \cdot 10^{-4}$

The tests are performed using a sensor with a wide frequency band (2-10 MHz), a defectoscope Panametrics and a spectral analyzer Textronics 2710. Spectra of successive echo-signals from the opposite side of a parallel-sided specimen are registered. The coefficient of attenuation within the material  $\alpha(f)$  is calculated using the relation

$$(13) \alpha(f) = \frac{1}{X} \left( \ln \frac{S_1}{S_2} \right),$$

where  $S_1$  and  $S_2$  are spectra of the first and second bottom signal and X is the acoustic path within the specimens.

Regarding the frequency range up to 12 MHz, coefficient  $\alpha(f)$  presents a sum of absorption and Rayleigh's scatter and it is written in the form

$$(14) \alpha(f) = \alpha_1 f + \alpha_4 f^4 = \alpha_1 f + C_R D^3 f^4,$$

where  $C_R$  is a structure coefficient depending on the material elastic properties and D is the grain mean diameter. An attenuation relation of Rayleigh's type ( $D/\lambda < 0.2$ ) is valid for the studied materials.

Fig. 15 shows spectra of specimens from groups 1 and 6 with notations  $\kappa - i$ , where  $\kappa$  is the group number and  $i$  is the number of the bottom signal. Fig. 16 presents attenuation coefficients (formula (13)) of specimens from groups 1, 4 and 6, found by averaging the results of several experiments. Values of the attenuation coefficient ( $\alpha_1$ ) and those of the scatter coefficient ( $\alpha_4$ ) are calculated and given in Table 1. A stronger attenuation within specimens with larger mean grain size is observed, which is in agreement with other publications, [7].

The results found confirm those found in other studies. They can serve as a basis in designing criteria for the estimation of material grain size.

The application of the method of spectral analysis yields increase of the accuracy and reliability of measurement of the ultrasonic wave attenuation coefficients.

## Conclusion

The paper presents model problems and experimental application of ultrasonic testing technique, using the method of spectral analysis. Computer modeling significantly facilitates the theoretical treatment of the problem and the performance of experiments. Moreover, it proves useful in the design of testing technologies and in qualifying ultrasonic non-destructive testing methods.

## Acknowledgement.

The study was sponsored by the Bulgarian Ministry of Education and Science, Contract No TH1303/2003.

## References

- [1] Ermolov, I. N., Theory and Practice of the Ultrasonic Testing, M., "Mashinostroenie", 1981 (Russian).

- [2] Mihovski, M., A Complex Use of Non-destructive Methods in the Study of the Structure and Physico-Mechanical Properties of Metallic Materials, D.Sc. Thesis, Institute of Mechanics, Bulg. Acad. Sci., 1991. (Bulgarian).
- [3] Mihovski, M., M. Lozev, Non-destructive Testing in Chemical Industry, S. "Tehnika", 1987 (Bulgarian).
- [4] Mekulova, V., V. Tokarev, Calculation of Wide-Band Piezo-Transducers for Ultrasonic Spectrometry and Immersion Defectoscopy, Defectoscopy, 1972, 4 (Russian).
- [5] Brehovskih, L. M., Waves in Layered Media, Publ. House of the USSR Acad. Sci., M., 1957 (Russian).
- [6] Truel, R., Ch. Elbaum, B. Chik, Ultrasonic Methods in Solid Physics, M., "Mir", 1972 (Russian).
- [7] Physical Acoustics, Ed. U. Meson, Vol. 4., B., M., "Mir", 1970 (Russian).
- [8] Hundigton H., On ultrasonic scattering by polycrystals, JASA, 1950, 22,3,362-369.
- [9] Mekulova, V. M., The Effect of Grain Distribution on Rayley's Scatter of Ultrasonic Waves, Defectoscopy, 1970, 2, 111-113 (Russian).
- [10] Ivanova, Y., Application of the Method of Spectral Analysis in Ultrasonic Investigations of Carbon Steels, National Conf. "Acoustics 2004", Sofia, 2004, 3-11 (Bulgarian).
- [11] Nagy P., L. Adler, Surface roughness induced attenuation of reflected and transmitted ultrasonic waves, JASA, 1987, 82,1, 193-197.



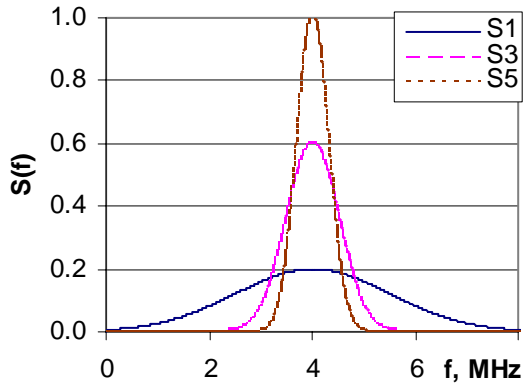


Fig. 1

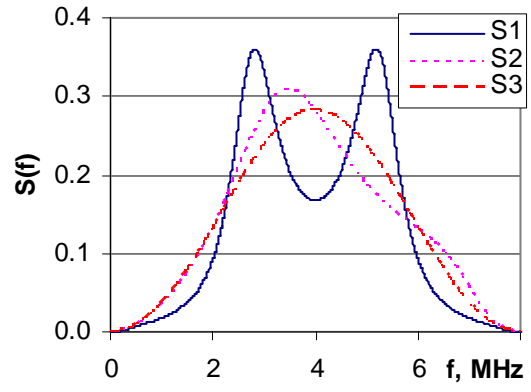


Fig. 2

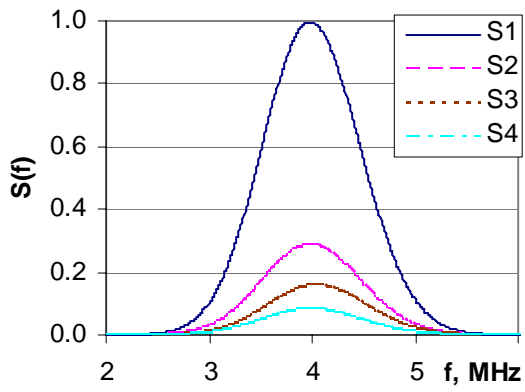


Fig. 3

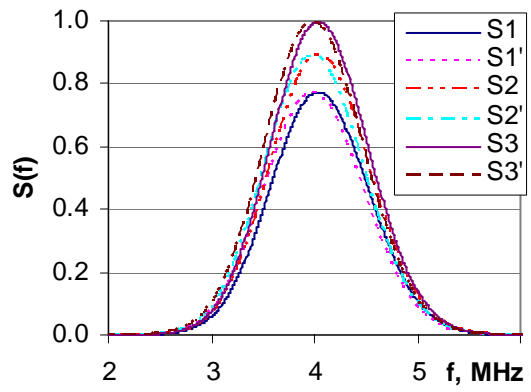


Fig. 4

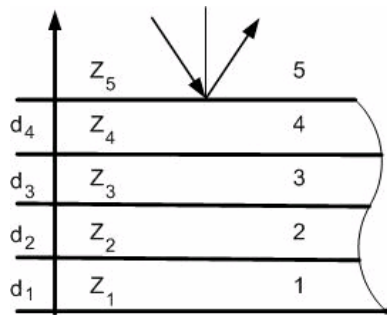


Fig. 5

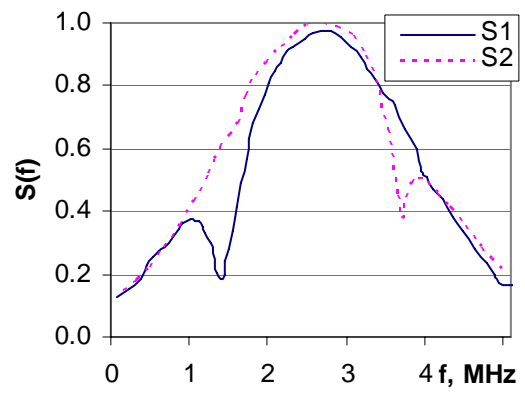


Fig. 6

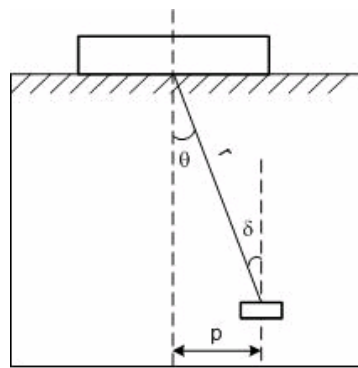


Fig. 7

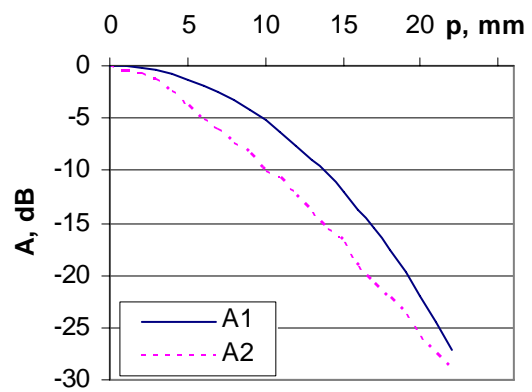


Fig. 8

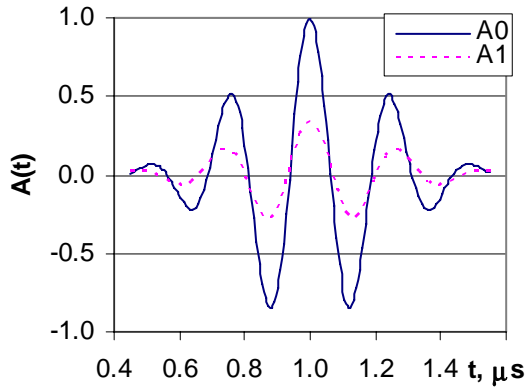


Fig. 9

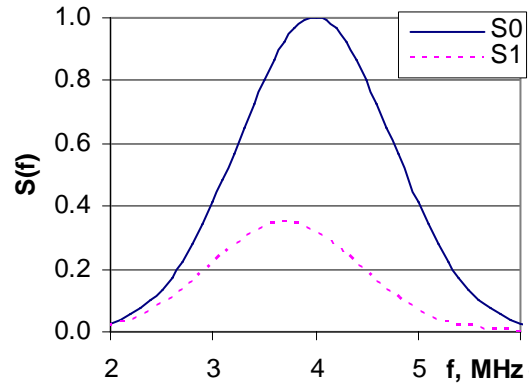


Fig. 10

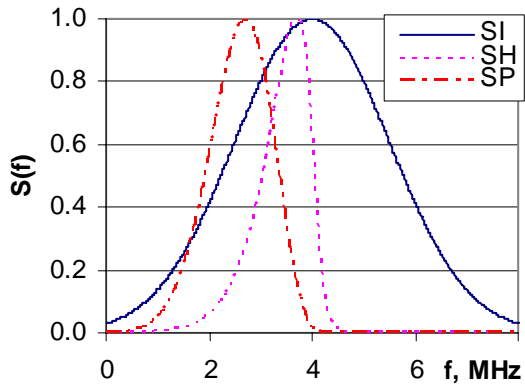


Fig. 11

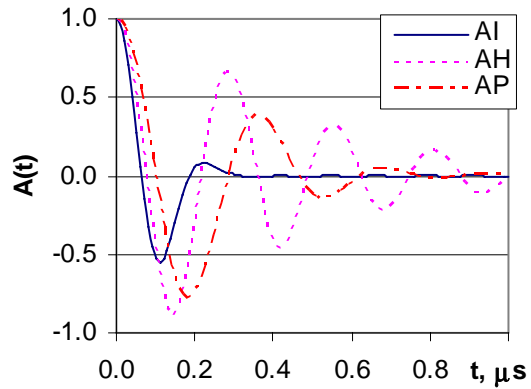


Fig. 12

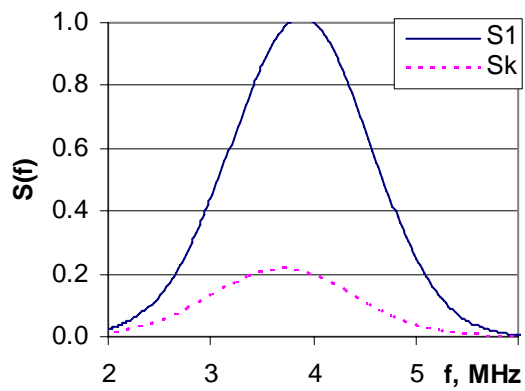


Fig. 13

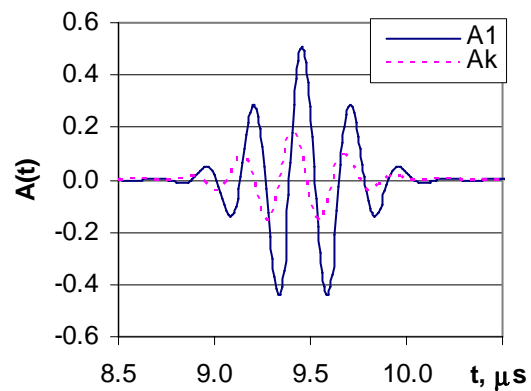


Fig. 14

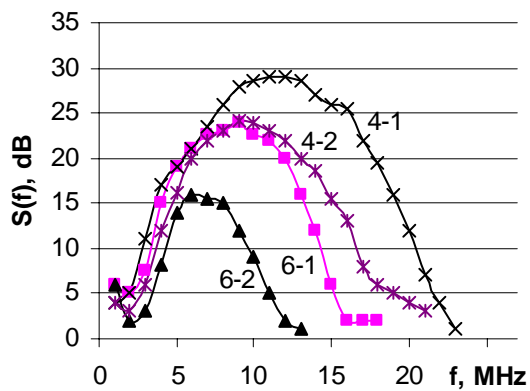


Fig. 15

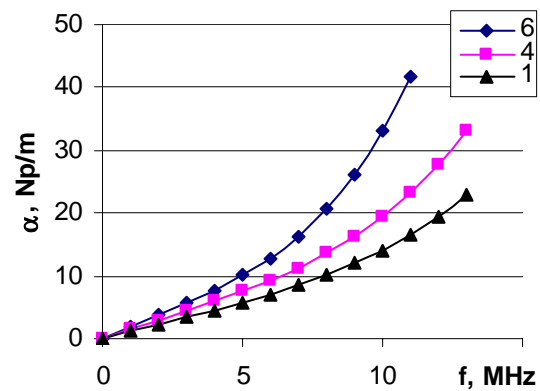


Fig. 16